

L-band ultrafast fiber laser mode locked by carbon nanotubes

Z. Sun,¹ A. G. Rozhin,¹ F. Wang,¹ V. Scardaci,¹ W. I. Milne,¹ I. H. White,¹ F. Hennrich,² and A. C. Ferrari^{1,a)}

¹Department of Engineering, University of Cambridge, Cambridge CB3 0FA, United Kingdom

²Institut für Nanotechnologie Forschungszentrum Karlsruhe, 76021 Karlsruhe, Germany

(Received 15 May 2008; accepted 18 July 2008; published online 15 August 2008)

We fabricate a nanotube-polyvinyl alcohol saturable absorber with a broad absorption at 1.6 μm . We demonstrate a pulsed fiber laser working in the telecommunication *L* band by using this composite as a mode locker. This gives $\sim 498 \pm 16$ fs pulses at 1601 nm with a 26.7 MHz repetition rate. © 2008 American Institute of Physics. [DOI: 10.1063/1.2968661]

The third telecommunications window around 1.55 μm , subdivided into conventional band (*C*, 1530–1565 nm) and long wavelength band (*L*, 1565–1625 nm),¹ is widely used in modern lightwave systems since the losses of silica fibers are lowest in this region.¹ Dense wavelength division multiplexed transmission systems are being developed to meet the rapidly growing data traffic demands.^{1,2} This makes the *L* band critical because it can be efficiently utilized to transport multiterabit traffic.² Ultrafast lasers in this spectral region can also find other applications, including spectroscopy,³ and biomedical diagnostics at frequency-doubled wavelengths.⁴ Passive mode-locked fiber lasers are practical alternatives to bulk laser systems due to their simplicity, compactness, efficient heat dissipation, and the ability to generate high-quality pulses.^{4–6} At present, semiconductor saturable absorber mirrors are typically used.^{4,7} However, they are typically complex and expensive quantum well devices, fabricated by molecular beam epitaxy on distributed Bragg reflectors.^{8,9} Ion implantation is typically required to reduce the recovery time.¹⁰ Novel nonlinear optical materials with better performance, cheaper fabrication, and easier integration are thus of great importance.

Recently, single wall nanotube (SWNT) based saturable absorbers have attracted considerable attention due to their outstanding properties, such as subpicosecond recovery time, low saturation power, broad operation range, polarization insensitivity, easy fabrication, and mechanical and environmental robustness.^{11–24} To date, SWNT-based saturable absorbers have been used to mode-lock fiber,^{12–21} waveguide,²² solid-state,²³ and semiconductor lasers.²⁴ These cover a broad range from 1 to 1.6 μm .^{12–24} Reference 21 reported a fiber laser working in the *L* band, mode locked by a 300 nm spray-coated SWNT layer with a peak absorption at 1550 nm. However, high losses due to the presence of large bundles and a significant intracavity dispersion²¹ strongly affected the output, resulting in large pulse widths and strong continuous wave background.

Here, we use a SWNT-polyvinyl alcohol (PVA) saturable absorber with a 340 nm wide absorption band peaked at 1600 nm to realize an ultrafast mode-locked erbium doped fiber (EDF) laser in the *L* band. This produces $\sim 498 \pm 16$ fs pulses with a repetition rate of 26.7 MHz at 1601 nm. This is the longest wavelength for which subpicosecond pulses

have been achieved thus far with SWNT-based saturable absorbers.

The band gap of the saturable absorber determines the device operation wavelength.²⁵ By tuning the deposition conditions, SWNTs with a specific diameter and gap distribution can be grown. This allows fine tuning of the absorption maximum and bandwidth. Here, we use SWNTs grown by laser ablation,²⁶ purified as described in Ref. 27. The diameter distribution is controlled by changing the growth temperature.^{12,26} 2 mg of SWNTs are dispersed in 14 ml water with 40 mg sodium dodecylbenzenesulphonate by using an ultrasonic processor (Nanoruptor, Diagenode). One part of SWNT solution is then mixed with three parts of 50% PVA aqueous solution. In order to remove residual bundles and impurities, the resulting solution is subjected to 40 000 g ultracentrifugation for 1 h. 50 μm thick freestanding films are then obtained drying at 45 °C in an oven. These have a homogeneous distribution of SWNTs on a submicron scale, as confirmed by a featureless surface in optical microscopy.

The composites are characterized by Raman spectroscopy and absorption spectrophotometry. From the radial breathing modes in the Raman spectra, we confirm that the films contain both metallic and semiconducting tubes with diameters from 1 to 1.4 nm. Their absorption is peaked at ~ 1600 nm, corresponding to the first transition in semiconducting tubes, with a bandwidth of ~ 340 nm, Fig. 1. The spectral features at ~ 900 nm and shorter wavelengths are the second and higher transitions.²⁸ The smooth and broad absorption band is due to presence of bundles.²⁹ A ~ 2 mm² composite is then sandwiched between two fiber-pigtailed

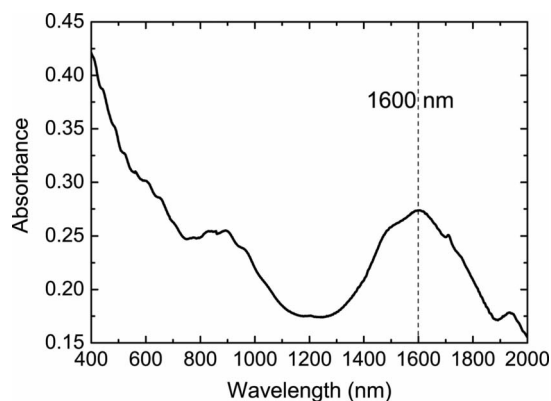


FIG. 1. Absorption spectrum of the SWNT-PVA film.

^{a)}Electronic mail: acf26@eng.cam.ac.uk.

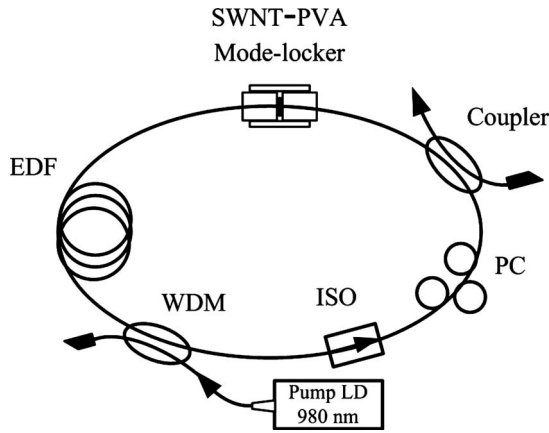


FIG. 2. Schematic setup of the mode-locked fiber laser. EDF denotes erbium doped fiber, WDM denotes wavelength division multiplexer, ISO denotes isolator, PC denotes polarization controller, and LD denotes laser diode.

connectors. An index matching gel is placed on both fiber ends to reduce propagation losses. The nonlinear absorption properties of the packaged film are characterized by power-dependent absorbance measurement with a commercial pulsed EDF laser (Toptica) at 1550 nm. This gives a saturation fluence of $\sim 13.9 \mu\text{J}/\text{cm}^2$ and a modulation depth of $\sim 16.9\%$. Such a high modulation depth provides a strong pulse shaping ability, which can lead to short pulse duration and reliable self-starting.³⁰

The packaged SWNT-PVA is then inserted into a fiber laser to generate mode-locked pulses, Fig. 2. The laser is in a ring configuration, using EDF as gain medium. A 2 m Liekki Er80–8/125 EDF is backward pumped by a 980 nm diode through a fused wavelength division multiplexer. Unidirectional

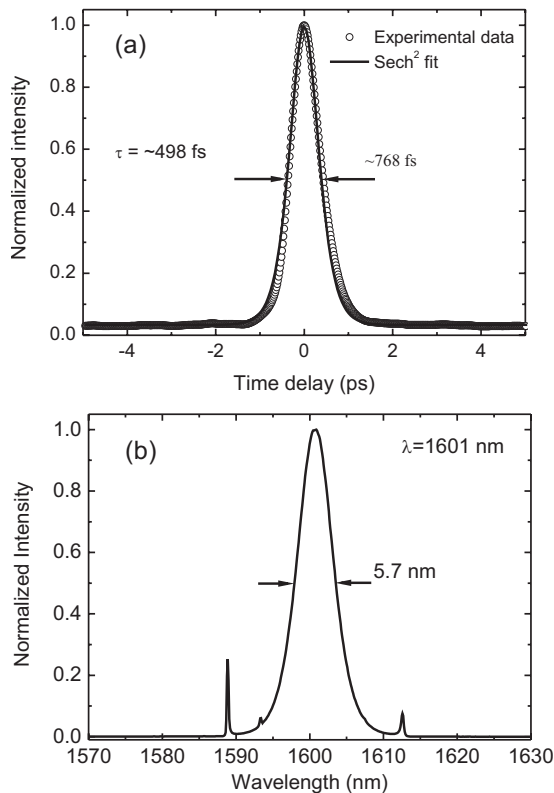


FIG. 3. (a) Autocorrelation trace. The time delay step is ~ 16 fs. (b) Typical output spectrum, centered at ~ 1601 nm, with bandwidth ~ 5.7 nm.

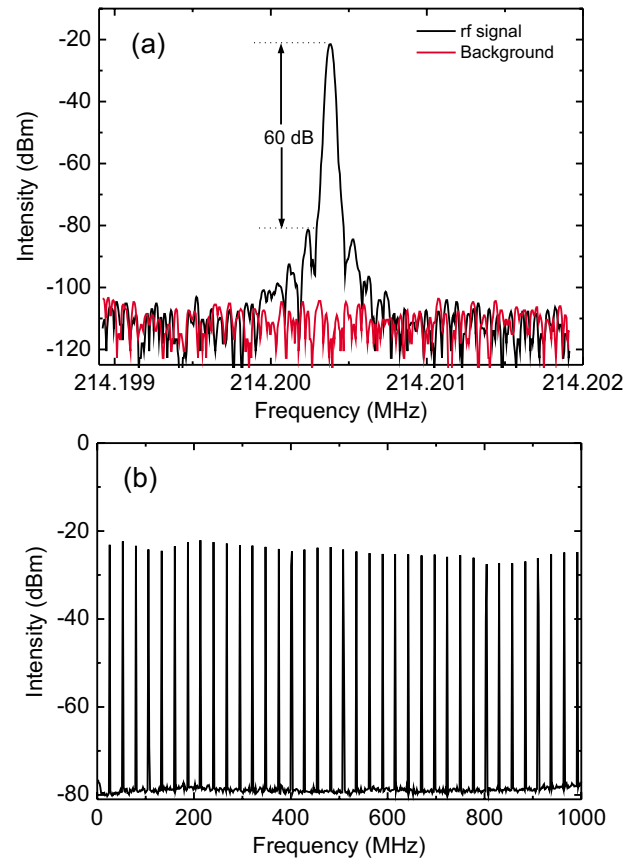


FIG. 4. (Color online) rf spectrum measured (a) around the eighth harmonic of the repetition rate, (b) over 1 GHz.

tional operation is ensured by an optical isolator. For mode-locking optimization, we adjust the polarization using an intracavity polarization controller. A fused 20/80 coupler is utilized as output coupler. The 80% port is selected to feed pulses back into the cavity. The total cavity length is estimated to be ~ 7.5 m. The pump power and average output power are measured by a photodiode power meter. Single-pulse operation is confirmed by a second harmonic generation (SHG) autocorrelator (Inrad 5–14-LDA) and by a 35 GHz high-speed sampling oscilloscope (Agilent Infiniium DCA). A spectrum analyzer (HP 86140A) with 0.1 nm resolution measures the output spectrum.

Continuous wave operation starts at 112 mW pump power. Self-starting stable single-pulse mode locking is observed at ~ 123 mW pump power with an average output power of 0.711 mW. The repetition rate is ~ 26.7 MHz, as determined by the cavity length. Single-pulse operation is observed up to 132 mW with average output power of 1.18 mW. Compared with previous C band nanotubes mode-locked EDF lasers,^{12–14} higher pump power is required to get continuous wave and mode-locked operation in the L band. This is because the EDF gain in the L band is approximately ten times lower than in the C band.³¹ Once started, the laser remains stable without need for temperature and vibration control.

Figure 3(a) plots a typical SHG autocorrelation trace, which is well fitted by a sech^2 temporal profile, resulting in a pulse duration of $\sim 498 \pm 16$ fs. Figure 3(b) shows a typical output pulse spectrum with central wavelength at ~ 1601 nm and bandwidth 5.7 nm. The sidebands at 1589 and 1613 nm are typical of solitonlike pulse formation³² which results

from intracavity periodical perturbation of discrete loss, gain, and dispersion.³² The time-bandwidth product (TBP) of the output pulses is 0.39 at an average output power of 1 mW. The deviation from the TBP value of 0.315 expected for transform-limited sech^2 pulses indicates the presence of minor chirping of the output pulses. Using the dependence of sideband wavelength on the dispersion and pulse width given in Ref. 32, we estimate an average intracavity group velocity dispersion ~ -19 ps²/km. Such cavity design favors soliton-like mode locking, which can provide a higher pulse quality.⁶ Even shorter pulses may be obtained using an additional intracavity group velocity dispersion compensation setup.³²

To study the operation stability, we measure the radio-frequency (rf) spectrum using an amplified lightwave converter connected to a spectrum analyzer with 30 Hz resolution. Figure 4(a) plots the rf spectrum around the eighth harmonic of the repetition rate. A signal-to-noise ratio of 60 dB is observed. Using the method of Ref. 33, we estimate the $\Delta T/T$ (T being the cavity round-trip time) $\approx 6.3 \times 10^{-5}$, corresponding to a low frequency jitter ΔT of 2.35 ps. We also perform measurements up to 1 GHz, Fig. 4(b). These show no spectrum modulation, implying no Q -switching instabilities.³⁴

In conclusion, we fabricated a SWNT-PVA saturable absorber with a broad absorption at 1600 nm and low saturation intensity. This is used as mode locker to generate $\sim 498 \pm 16$ fs pulses with a repetition rate of 26.7 MHz at 1601 nm. This can lead to novel ultrafast light sources to meet the application requirements in the L band.

We thank Liekki for EDF. We acknowledge funding from EPSRC (GR/S97613/01 and EP/E500935/1), the Leverhulme and Isaac Newton trusts, and The Royal Society.

¹G. P. Agrawal, *Lightwave Technology: Telecommunication Systems* (Wiley, New Jersey, 2005).

²A. K. Srivastava, S. Radic, C. Wolf, J. C. Centanni, J. W. Sulhoff, K. Kantor, and Y. Sun, *IEEE Photonics Technol. Lett.* **12**, 1570 (2000).

³J. Marshall, G. Stewart, and G. Whitenett, *Meas. Sci. Technol.* **17**, 1023 (2006).

⁴O. Okhotnikov, A. Grudinin, and M. Pessa, *New J. Phys.* **6**, 177 (2004).

⁵M. E. Fermann, A. Galvanauskas, G. Sucha, and D. Harter, *Appl. Phys. B: Lasers Opt.* **65**, 259 (1997).

⁶L. E. Nelson, D. J. Jones, K. Tamura, H. A. Haus, and E. Ippen, *Appl. Phys. B: Lasers Opt.* **65**, 277 (1997).

⁷H. Sotobayashi, J. T. Gopinath, E. M. Koontz, L. A. Kolodziejski, and E. P. Ippen, *Opt. Commun.* **237**, 399 (2004).

⁸U. Keller, K. J. Weingarten, F. X. Kärtner, D. Kopf, B. Braun, I. D. Jung,

R. Fluck, C. Hönniger, N. Matuschek, and J. A. D. Au, *IEEE J. Sel. Top. Quantum Electron.* **2**, 435 (1996).

⁹S. Suomalainen, A. Vainionp, O. Tengvall, T. Hakulinen, S. Karirinne, M. Guina, O. G. Okhotnikov, T. G. Euser, and W. L. Vos, *Appl. Phys. Lett.* **87**, 121106 (2005).

¹⁰E. Lugagne Delpon, J. L. Oudar, N. Bouche, R. Raj, A. Shen, N. Stelmakh, and J. M. Lourtioz, *Appl. Phys. Lett.* **72**, 759 (1998).

¹¹Y. C. Chen, N. R. Ravivkar, L. S. Schadler, P. M. Ajayan, Y. P. Zhao, T. M. Lu, G. C. Wang, and X. C. Zhang, *Appl. Phys. Lett.* **81**, 975 (2002).

¹²S. Y. Set, H. Yaguchi, Y. Tanaka, and M. Jablonski, *IEEE J. Sel. Top. Quantum Electron.* **10**, 137 (2004).

¹³M. Nakazawa, S. Nakahara, T. Hirooka, M. Yoshida, T. Kaino, and K. Komatsu, *Opt. Lett.* **31**, 915 (2006).

¹⁴F. Wang, A. G. Rozhin, Z. Sun, V. Scardaci, I. H. White, and A. C. Ferrari, *Phys. Status Solidi B* (to be published).

¹⁵A. G. Rozhin, Y. Sakakibara, S. Namiki, M. Tokumoto, H. Kataura, and Y. Achiba, *Appl. Phys. Lett.* **88**, 051118 (2006).

¹⁶S. Yamashita, S. Y. Set, C. S. Goh, and K. Kikuchi, *Electron. Commun. Jpn., Part 2: Electron.* **90**, 17 (2007).

¹⁷V. Scardaci, A. G. Rozhin, F. Hennrich, W. I. Milne, and A. C. Ferrari, *Physica E (Amsterdam)* **37**, 115 (2007).

¹⁸V. Scardaci, A. G. Rozhin, P. H. Tan, F. Wang, I. H. White, W. I. Milne, and A. C. Ferrari, *Phys. Status Solidi B* **244**, 4303 (2007).

¹⁹Y. W. Song, S. Yamashita, and S. Maruyama, *Appl. Phys. Lett.* **92**, 021115 (2008).

²⁰A. G. Rozhin, V. Scardaci, F. Wang, F. Hennrich, I. H. White, W. I. Milne, and A. C. Ferrari, *Phys. Status Solidi B* **243**, 3551 (2006).

²¹S. Yamashita, Y. Inoue, H. Yaguchi, M. Jablonski, and S. Y. Set, European Conference on Optical Communication 2004, Paper No. Th.1.3.4.

²²G. Della Valle, R. Osellame, G. Galzerano, N. Chiodo, G. Cerullo, P. Laporta, O. Svelto, U. Morgner, A. G. Rozhin, V. Scardaci, and A. C. Ferrari, *Appl. Phys. Lett.* **89**, 231115 (2006).

²³K. H. Fong, K. Kikuchi, C. S. Goh, S. Y. Set, R. Grange, M. Haiml, A. Schlatter, and U. Keller, *Opt. Lett.* **32**, 38 (2007).

²⁴Y. W. Song, S. Yamashita, C. S. Goh, and S. Y. Set, *Opt. Lett.* **32**, 430 (2007).

²⁵E. Garmire, *IEEE J. Sel. Top. Quantum Electron.* **6**, 1094 (2000).

²⁶S. Lebedkin, P. Schweiss, B. Renker, S. Malik, F. Hennrich, M. Neumaier, C. Stoermer, and M. M. Kappes, *Carbon* **40**, 417 (2002).

²⁷F. Hennrich, R. Wellmann, S. Malik, S. Lebedkin, and M. M. Kappes, *Phys. Chem. Chem. Phys.* **5**, 178 (2003).

²⁸H. Kataura, Y. Kumazawa, Y. Maniwa, I. Umezumi, S. Suzuki, Y. Ohtsuka, and Y. Achiba, *Synth. Met.* **103**, 2555 (1999).

²⁹P. H. Tan, A. G. Rozhin, T. Hasan, P. Hu, V. Scardaci, W. I. Milne, and A. C. Ferrari, *Phys. Rev. Lett.* **99**, 137402 (2007).

³⁰R. Herda, O. G. Okhotnikov, E. U. Rafailov, W. Sibbett, P. Crittenden, and A. Starodumov, *IEEE Photonics Technol. Lett.* **18**, 157 (2006).

³¹Y. Shiquan, Z. Chunliu, M. Hongyun, D. Lei, D. Xiaoyi, Y. Shuzhong, K. Guiyun, and Z. Qida, *Opt. Quantum Electron.* **35**, 69 (2003).

³²M. L. Dennis and I. N. Duling, *IEEE J. Quantum Electron.* **30**, 1469 (1994).

³³D. Linde, *Appl. Phys. B: Lasers Opt.* **39**, 201 (1986).

³⁴C. Honninger, R. Paschotta, F. Morier-Genoud, M. Moser, and U. Keller, *J. Opt. Soc. Am. B* **16**, 46 (1999).